Accepted in The Astrophysical Journal

Low Surface Brightness Galaxies in the SDSS: the link between environment, star-forming properties and AGN

Gaspar Galaz, Rodrigo Herrera-Camus[1]

Departamento de Astronomia y Astrofisica, Pontificia Universidad Catolica de Chile

ggalaz@astro.puc.cl, rhc@astro.umd.edu

Diego Garcia-Lambas

Consejo Nacional de Investigaciones Cientificas y Tecnicas, Argentina, IATE, CONICET, OAC, Universidad Nacional de Cordoba, Argentina

dgl@mail.oac.uncor.edu

and

Nelson Padilla

Departamento de Astronomia y Astrofisica, Pontificia Universidad Catolica de Chile

npadilla@astro.puc.cl

ABSTRACT

Using the Sloan Digital Sky Survey (SDSS) data release 4 (DR 4), we investigate the spatial distribution of low and high surface brightness galaxies (LSBGs and HSBGs, respectively). In particular, we focus our attention on the influence of interactions between galaxies on the star formation strength in the redshift range $0.01 < z < 0.1$. With cylinder counts and projected distance to the first and fifth-nearest neighbor as environment tracers, we find that LSBGs tend to have a lack of companions compared to HSBGs at small scales (< 2 Mpc). Regarding the interactions, we have evidence that the fraction of LSBGs with strong star formation activity increases when the distance between pairs of galaxies (r_p)

[1]Present address: Department of Astronomy, University of Maryland at College Park, USA.

is smaller than about four times the Petrosian radius (r_{90}) of one of the components. Our results suggest that, rather than being a condition for their formation, the isolation of LSBGs is more connected with their survival and evolution. The effect of the interaction on the star formation strength, measured by the average value of the birthrate parameter b, seems to be stronger for HSBGs than for LSBGs. The analysis of our population of LSBGs and HSBGs hosting an AGN show that, regardless of the mass range, the fraction of LSBGs having an AGN is lower than the corresponding fraction of HSBGs with an AGN. Also, we observe that the fraction of HSBGs and LSBGs having an AGN increases with the bulge luminosity. These results, and those concerning the star-forming properties of LSBGs as a function of the environment, fit with the scenario proposed by some authors where, below a given threshold of surface mass density, low surface brightness disks are unable to propagate instabilities, preventing the formation and evolution of massive black holes in the centers of LSBGs.

Subject headings: Astronomical databases: catalogs — Galaxies: general — Galaxies: star formation — Galaxies: statistics — Galaxies: stellar content

1. Introduction: new questions

Low surface brightness galaxies (LSBGs hereafter) represent an important population among extragalactic objects. In particular, spiral LSBGs are characterized by a disk surface brightness at least one order of magnitude lower than the canonical value of 21.65 mag arcsec^{-2} proposed by Freeman (1970). The central surface brightness of the disk in the B-band, $\mu_0(B)$, is the photometric parameter typically used to distinguish between the high and the low surface brightness regime of galaxies. The most common threshold values found in the literature are between 22 and 23 mag arcsec^{-2} (Impey et al. 2001, among others). Although LSBGs share many of the properties also found in high surface brightness galaxies (HSBGs), they also present a significant list of challenging observational features. Just to mention the most intriguing ones (some of them will be explained more extensively in the next paragraph), they have a very low stellar density (which actually produces the low surface brightness), but exhibit astonishing flat rotation curves, reaching large radii from the center of the galaxy (de Blok 2005; Swaters, Sanders & McGaugh 2010). This implies that LSBGs are one of the most dark matter dominated systems in the Universe, given their high M/L ratio (Sprayberry et al. 1995a). Another striking feature in LSBGs is the richness of their stellar populations, which span the whole range of the HR-diagram (Zackrisson, Bergvall & Ostlin 2005; Zhong et al. 2008), challenging the extraordinary deficit

in molecular gas, as detected so far (O'Neil, Hofner & Schinnerer 2000; Matthews & Gao 2001; Galaz et al. 2008). Finally, the low star formation rate (SFR) in combination with their rather isolated location in the cosmic web (Rosenbaum et al. 2009), as reported by several authors (see below), give clues for the understanding of their formation and evolution.

Among the mentioned properties, we highlight three of them related with the purpose of this work. First, it seems that LSBGs evolve following a similar track of high surface brightness galaxies (HSBGs), but with a significantly slower rate of star forming processes (van den Hoek et al. 2000). Second, systematic evidence shows that LSBGs are strongly dominated by dark matter (de Blok et al. 1996). Then, far from being fragile, simulations suggest that disks of LSBGs would be very stable against the propagation of gravitational instabilities which are typically generated by interactions with, for example, a close neighbor (Mihos et al. 1997; Mayer & Wadsley 2004). Finally, LSBGs would be more isolated than HSBGs at small scales (less than 2 Mpc), according to Bothun et al. (1993), and between 2 Mpc and 5 Mpc (Rosenbaum et al. 2009). These last results motivate the following question: is the isolation of LSBGs a requisite for their formation or for their subsequent evolution? In other words, if the reaction of LSBGs to close interactions results in the enhancement of their star formation activity, as has been previously observed in HSBGs (Lambas et al. 2003; Nikolic et al. 2004), then the lack of tidal encounters in a Hubble time, because of their isolation, could explain the less evolved nature of LSBGs respect to HSBGs (Bothun et al. 1987). On the other hand, if LSBGs are strongly influenced by the interactions, then the isolation would indicate a fast transition from an LSB regime to the HSB regime in high density environments.

In an effort to better understand the relationship between the spatial distribution of LSBGs and their star formation properties, we focus our attention in a carefully selected sample of this kind of galaxies extracted from the Sloan Digital Sky Survey (SDSS) data release 4 (DR 4) (Abazajian et al. 2004), as well as in a similarly selected control sample of high surface brightness galaxies from the same catalog. Along with the analysis of the degree of isolation of LSBGs, we will focus our attention on the possible relationship between the local density and their star-formation properties, including the behavior of LSBGs in pairs.

The paper is organized as follows. In §2 we describe the galaxy selection from the SDSS DR 4 and the corrections applied to such a selection, showing also some basic relationships; in §3 we define the density estimators to be used in the analysis, as well as the tools to define galaxy pairs. In §4 we analyse the most important results regarding the environment and the star-formation properties of LSBGs, including an analysis of the LSB population exhibiting an AGN. We discuss our results within the scope of the recent work by other authors in §5. Finally, we summarize our conclusions in §6.

2. The sample

2.1. Selecting low surface brightness galaxies from the SDSS

The galaxies studied in this work were extracted from the Main Galaxy Sample (Strauss et al. 2002) of the SDSS data release 4 (DR 4). Following a similar procedure to that presented by Zhong et al. (2008), we select preferentially late type galaxies ($fracDev_r \leq 0.9$)[1] with spectroscopically computed redshifts, nearly face-on to avoid serious extinction correction ($b/a > 0.4$), not too nearby to avoid problems with peculiar velocities ($z \geq 0.01$) and, to avoid serious incompleteness effects, not too distant ($z \leq 0.1$, see also Rosenbaum et al. 2009). Note that Zhong et al. (2008), using also the SDSS, selected galaxies with $fracDev_r \leq 0.25$. In spite that this last figure seems to be quite different than our selection criteria, we realize that most of the LSBGs included in our sample (86%) do have $fracDev_r \leq 0.25$. It is worth noting that recently, Rosenbaum et al. (2009) did an excellent work selecting LSBGs from the same catalog (DR 4), and concluded that the SDSS is biased to select two different kinds of galaxies in two different redshift intervals, $0.010 < z < 0.055$ and $0.055 < z < 0.100$, which span our redshift selection. In the first redshift range, most of the LSBGs are dwarf-type galaxies, LMC-like. In the second redshift range, the majority of galaxies are massive, well defined spiral systems (where in fact one can very well define a disk and bulge). With our luminosity profile selection ($fracDev_r \leq 0.90$) we are only loosing some extreme LSBGs with a huge bulge component and very faint disks (i.e. galaxies where the de Vaucouleurs component contributes more than 90% of the total light). On the other hand, irregular galaxies enter in our catalog if an exponential light profile is possible to be fitted, which is the case for about 95% of the cases in the spectroscopic catalog. Therefore, comparisons between this work and the one by Rosenbaum et al. (2009) can in principle be made. In fact, further in the text it is possible to conclude that our results regarding the large-scale distribution and the distribution of LSBGs in terms of the local density, agree well with Rosenbaum et al..

Since the spectroscopic catalog of the SDSS is a magnitude-limited survey ($r \leq 17.77$ mag), the observed populations of galaxies are not the same as the redshift increases. In fact, when going farther in redshift, a magnitude-limited selection introduces a strong bias selecting more luminous (and massive) galaxies. This prevents us to compare in a statistical way nearby galaxies with galaxies situated at higher redshifts. Therefore, one has to define a redshift range (i.e. a volume and a lower luminosity limit) where the absolute magnitude distributions are the same for all the galaxy populations. A volume-limited catalog allows

[1]The *fracDev* parameter in the SDSS refers basically to the fraction of the light coming from a fitted de Vaucouleurs light profile.

us to compare two populations of LSBGs and HSBGs having roughly the same absolute magnitude range and therefore with roughly the same mass cuts, as we show in furthers sections. Another way to correct for the bias from a magnitude-limited catalog is to use the V/V_{max} approach, which will also be used (see the end of §2.3).

2.2. Magnitude conversion and surface brightness

Since the criterion for LSB classification is done in the Johnson B band, and the SDSS filters does not include it, we are forced to transform the SDSS g and r magnitudes into B-Johnson magnitudes. Using information derived from the fit of a pure exponential profile included in the SDSS data, we calculate the surface brightness in the g- and r-band. Then, from the conversions of Smith et al. (2002), we get the surface brightness in the B-band, which is computed as

$$\mu_0(m) = m + 2.5log(2\pi a^2) + 2.5log(b/a) - 10log(1+z), \quad (1)$$

where m is the apparent magnitude in the B band, the second factor is the area where the light is measured (enclosing 90% of the light), the third factor is the inclination correction (where a is the semi-major axis, b is the minor axis) assuming a disk of uniform radiance, and the fourth factor is the surface brightness correction for the cosmological dimming (the well-known $(1+z)^{-4}$ factor). The a and b parameters are defined from the photometric exponential fit to the galaxy

Using a surface brightness cut value of $\mu_0(B) = 22.5$ mag arcsec^{-2}, we select a sample of 9,421 LSBGs from the complete spectroscopic catalog of 567,486 galaxies, i.e. 1.66% of the galaxies of the total sample are LSBGs. These galaxies satisfy the surface brightness cut and also the redshift, inclination and morphology constraints specified in §2.1. Applying the same redshift cuts and imposing the same spectroscopic flags as for the LSB sample, we select 30,000 HSB galaxies. In addition to the Sloan spectroscopic information, we have added information from Brinchmann et al. (2004), which includes the star formation rate, the estimated stellar mass for each galaxy (M_*) and the 4000 Å break index (D_n4000). Also, with the aim to flag galaxies hosting an active galactic nucleus (AGN), we cross-correlate our catalog with that of Kauffmann et al. (2003). These galaxies have to be excluded from our analysis when studying the light and colors supposedly coming from canonical star forming processes. Therefore, if one excluded galaxies with AGN, then the number of LSBGs is

reduced to 8,926 and the number of HSBGs to 24,324[2]. Specific studies of AGN are presented in a forthcoming paper (however, see §4.3).

2.3. Volume corrections

In order to correct the bias introduced from the differences in both the redshift and absolute magnitude distributions for the HSBGs and LSBGs, we weight the fractions and averages with the inverse of the maximum volume out to which each galaxy can be detected in the SDSS (i.e. we use the V/V_{max} method, Schmidt 1968). Figure 1 shows the relationship between the absolute magnitude, the Petrosian radius ${r_{90}}^3$ and the exponential scale-length, for HSBGs (in black) as well as for LSBGs (in red). This Figure clearly presents the combined bias resulting from two selection functions, namely, the strong dependence of the absolute magnitude vs. redshift in the SDSS spectroscopic catalog (a magnitude-limited catalog), and the trend of the absolute magnitude on the galaxy size. By weighting each galaxy for its accessible volume using the factor V/V_{max}, we correct the effective fractions of galaxies, specially the few ones detected at faint absolute magnitudes (the bottom edge in Figure 1). Figure 1 clearly shows that for a given absolute magnitude, LSBGs are larger than HSBGs. Note that our sample of galaxies also includes some irregular galaxies, but not the usually faint ones. These have small values of fracDev (< 0.2) and faint absolute magnitudes (usually $M_r > -16.0$, see Figure 1). Given that our spectroscopic catalogue is a magnitude limited catalog with with $m_r \leq 17.77$ mag, these galaxies are visible only up to $z \sim 0.01$, which is exactly the redshift we start to consider for this study. Then we do not detect these faint irregulars. To have an idea about how many irregulars are we loosing up to such a redshift we first selected the total number of LSBGs and HSBGs up to $z = 0.01$, which gives 741 and 1099 respectively. From these, about 30% are galaxies of small Petrosian radius (smaller than 2 kpc). This fraction is about the same for the low surface brightness and the high surface brightness population, as shown by the solid and dashed lines of the histogram. If irregulars are represented by these galaxies, that means that we are loosing a 40% of the total sample, which is a significant fraction. However, only 30% of them are fainter than $M_r < -16.0$. Also, it is well known that there are also LSBGs with small radius and not necessarily irregulars, for example dwarf galaxies that enter into our sample (de Lapparent et al. 2004). So the fraction of irregulars is probably smaller than 40%. To be sure, we have examined in detail the number of irregulars at $z \leq 0.01$ that are included

[2]The HSB number of galaxies is only a sub-sample of the total sample build as a control sample.

[3]The equivalent circular radius enclosing 90% of the galaxy light, in the r-band.

in the sample of 741 LSBGs up to $z \sim 0.01$. We found, *by eye*, that 127 (17%) of these are clearly irregulars. A significant number of galaxies, about the same fraction, are dwarf systems with sizes ~ 15 kpc or smaller.

Figure 2 shows the distribution of properties extracted from our sample of LSBGs and HSBGs, considering the V/V_{max} weight. Looking at the two upper histograms, we observe indeed that LSBGs (in red) and HSBGs (in black) do not have the same redshift and absolute magnitude distributions. This Figure is consistent with Figure 1 in Rosenbaum et al. (2009). The middle panels in Figure 2 show the fractional histograms for the stellar mass and the star formation rate, for HSBGs and LSBGs, weighted by the V/V_{max} factor. We see that LSBGs peak at slightly less massive objects compared to HSBGs, and also with a broader mass distribution. A similar result is observed for the SFR distribution (right panel), where the LSBGs peak at about 0.9 $M_\odot$/yr, compared to HSBGs, which in average form more stars per year, 1.8 $M_\odot$/yr, as expected. The two bottom panels show the distributions of the birthrate parameter b and the Petrosian radius, respectively. The birthrate parameter is defined as

$$b = (1 - R) t_H \frac{SFR}{M_\star}, \tag{2}$$

where R is the total stellar mass fraction which is ejected to the interstellar medium (ISM) during the lifetime of the galaxy, t_H is the Hubble time, and the ratio SFR/M_* is the star formation rate (SFR) per unit of solar mass (also called specific SFR[4]). Usually R is set as 0.5 (Brinchmann et al. 2004). Interestingly, Figure 2 shows that LSBGs and HSBGs have the same birthrate parameter distribution, when corrected by the V/V_{max} factor. Also, the right histogram shows that LSBGs and HSBGs have clearly different Petrosian radius r_{90} distributions, both in range and peak values.

2.4. Volume-limited sample

All the distributions shown in Figure 2 are slightly modified if one directly uses a volume-limited sample of galaxies, instead of the V/V_{max} weighted distributions. However, even though the absolute magnitude-redshift bias is eliminated, the number of galaxies is small. Another drawback of having a volume-limited sample is that the catalog now includes preferentially bright galaxies, in our case galaxies brighter than $M_r = -19.8$ mag. When

[4]The specific SFR is usually a better estimator than the SFR for the actual amount of mass which forms stars in a given galaxy, since it is the SFR per unit of galaxy mass.

this cut in absolute magnitude is used, the total number of LSBGs is reduced to 1,110, and the corresponding number of HSBGs to 7,526. Figure 3 shows the same histograms as Figure 2 but for the volume-limited sample. We see that most of them are consequently modified, especially the redshift and absolute magnitude distributions, as expected. The middle panel of Figure 3 shows that now the two populations do have more similar stellar mass distributions (easily understood from the now similar absolute magnitude distribution), although LSBGs still have lower masses.

Also, now the birthrate distributions for LSBGs and HSBGs are no longer the same. Indeed as expected, LSBGs form in average, less solar masses per year, during their lifetime. That could be interpreted as the fact that although LSBGs and HSBGs could have the same stellar formation history, LSBGs form stars in a longer periods of time.

Finally, the right bottom panel indicate that the Petrosian radius distributions are not only still different, as expected from the definition itself of low surface brightness, but are markedly different, both in peak values and in range.

Table 1 shows the averaged quantities studied in Figure 2 and 3 for LSBGs as well as for HSBGs. In average, LSBGs with the same average total absolute magnitudes of the HSB counterparts, have the same stellar mass, but form 8 times less solar masses per year, and are 1.5 times larger than HSBGs. Note also that the average b parameter is higher in HSBGs than in LSBGs, for the two ways of weighting galaxies. In particular, for the volume limited sample, LSBGs form almost 10 times less stars per unit mass than HSBGs.

3. Density estimators and pair recognition

In this section we briefly define the density estimators that will be used to analyze the degree of isolation of our sample of LSBGs. We also define the parameters and criteria to define our sample of pairs.

We use two methods to estimate the spatial density of galaxies: (1) the object counting in a fixed aperture over the sky, and (2) the distance to the n^{th}-closest neighbor for a given galaxy. In both cases, we only use the galaxies included in the volume-limited sample ($M_r \leq -19.8$).

In the first method, also used by Bothun et al. (1993) for 340 LSBGs, and recently by Rosenbaum et al. (2009), we count the number of galaxies in cylinders of fixed height ($\pm$500 km/s) and radii up to 5 Mpc in steps of 0.25 Mpc, to calculate the surface density of galaxies inside each cylinder. For a given galaxy the number of neighbors included in each cylinder

allows to define a surface density of galaxies as a function of radius, which in turn can be used to define its local density.

In the second method, we compute both the projected distance to the nearest neighbor r_p (i.e. $N = 1$) within a velocity shell of $\pm$500 km/s, and the projected distance to the fifth nearest neighbor d_5 ($N = 5$), brighter than the K-corrected absolute magnitude $M_r = -19.8$, and within a velocity range of $\pm$500 km/s. This last estimator allows us to characterize the local environment around the target galaxy by means of the well-known surface density parameter Σ_5 (Rosenbaum et al. 2004; Balogh et al. 2004; Alonso et al. 2006; Padilla, Lambas & González 2010) defined by

$$\Sigma_5 = \frac{5}{\pi d_5^2}, \tag{3}$$

where d_5 is the projected distance to the 5^{th}-closest and brighter than $M_r = -19.8$ mag neighbor.

4. Results

4.1. How isolated are LSBGs? Environment around LSBGs

In this section we analyze the spatial distribution of the volume-limited sample of LSBGs and HSBGs, using the two estimators defined in §3. Figure 4 shows the cumulative distribution of r_p (left panel) and d_5 (right panel) for both LSBGs (red lines) and HSBGs (black lines). It is apparent from this Figure that for both neighbor definitions, LSBGs are more isolated than HSBGs, specially at scales smaller than 5 Mpc. Indeed, at a fixed cumulative fraction, LSBGs tend to have the fifth nearest neighbor *farther* away than HSBGs, in the region $0.5 \leq r \leq 2$Mpc for r_p and almost the full range of scales shown for d_5 ($0.5 \leq r \leq 10$Mpc). A Kolmogorov-Smirnov (K-S) test rejects, with high level of confidence (99%), the hypothesis that the distance distribution is the same for both samples of galaxies. This behavior is still more apparent for scales smaller than 2 Mpc. Note that we do not observe a significant degree of isolation in LSBGs at intermediate scales as described by Rosenbaum et al. (2004, 2009), probably because we are using a volume-limited sample.

When using the cylinder estimator one gets the same results as with the nearest first and fifth neighbor. A better estimator of the degree of isolation of galaxies, other than the pure cylinder counts, is the surface density of galaxies around a given target galaxy (Σ_5). This estimator is shown in Figure 5, where it is apparent that LSBGs (red) have a lower number of companions than HSBGs (black), specially at scales smaller than 1.5 Mpc. The

percentage of galaxies without neighbors at $r < 0.5$ Mpc is $76 \pm 2\%$ for LSBGs and $70 \pm 1\%$ for HSBGs. Note that high density environments are not exclusively inhabited by HSBGs. Nearly 7% of LSBGs have 8 or more neighbors at $r < 2.0$ Mpc, compared to $\sim 10\%$ for the HSB case.

Note that all the above indicators show that on average LSBGs are more isolated than HSBGs. However, it is worth noting that although the last affirmation is correct, it is also true that some LSBGs are also located in dense environments, in particular in groups and pairs, as will be discussed in §4.2.

With the aim to characterize the extremes of the local density as populated by LSBGs, we follow the same convention as Bothun et al. (1993), who defined *isolated* galaxies as those having no neighbors up to a distance of 2 Mpc. On the other hand, galaxies having 8 or more neighbors up to the same radius of 2 Mpc, are defined as *populars*. Using this criterion, 14%±2% and 18%±2% of LSBGs in our sample are classified as isolated and populars, respectively. Interestingly, a similar fraction of isolated HSB galaxies is found (13%±1%). However, the fraction of popular galaxies for HSBGs is clearly larger than for LSBGs: 23%±1%. Therefore, this approach indicates that LSBGs are not necessarily more isolated than HSBGs, but less "sociable" at scales smaller than 2 Mpc. Our results are in excellent agreement with those early results by Bothun et al. (1993) for their small sample of 340 LSBGs.

4.2. Properties of star-forming LSBGs as a function of the environment: LSBGs in pairs

Among the many issues regarding the formation and evolution of LSBGs, their (deficient) star forming properties as a function of the environment is one of the most unexplored. The conclusion of §4.1 could hold clues about the elusive connection between the local density and the star-formation properties of LSBGs. From Table 2, which includes averaged values for the absolute magnitude, color, the birthrate parameter b and D_n4000, we are unable to conclude that environment variations can produce a significant difference on the stellar formation activity between LSBGs and HSBGs, at least on the scales included in the Table. It is worth to note that we have excluded AGN galaxies from the analysis, using the AGN catalog by Kauffmann et al. (2003) (see §4.3). If the environment has a different influence on the stellar formation activity in LSBGs and HSBGs, such an influence should be seen at small scales, where interactions between galaxies take place.

To investigate the impact of interactions on the star forming properties on both LSBGs

and HSBGs, we built a sample of pairs from the main LSB and HSB catalogs. The pairs sample is built using limits on the radial velocity differences (ΔV) between the central galaxy and its first neighbor, and the projected distance in Mpc (r_p) normalized by the galaxy radius (here r_{90}, in kpc in the r band). This is the same approach as used in Lambas et al. (2003), and Alonso et al. (2006), allowing to measure the distance to the corresponding companion in terms of the influence radius of a galaxy. We note that the close neighbor of a given target LSB or HSB galaxy is extracted from the whole spectroscopic SDSS database, not necessarily included in our constrained catalogs of LSBGs and HSBGs. This means that the neighbor can have any morphology, surface brightness, color or magnitude (both apparent or absolute). The catalog of pairs is composed by galaxies that satisfy, along with the neighbor galaxy, only two constraints: $\Delta V \leq 500$ km/s, and $r_p/r_{90} \leq 10$. The number of pairs selected for the sample without cuts in absolute magnitude turns out to be 268 and 868 for LSBGs and HSBGs, respectively. If we only consider galaxies with a cut in absolute magnitude (i.e. galaxies with $M_r \leq -19.8$ mag) then the number of pairs where the target galaxy is an LSB decreases to only 67 pairs. This number is too small to extract statistical properties. Therefore, for this analysis we use the complete sample of LSBGs and HSBGs, without any cut in absolute magnitude, but correcting statistically the counts by the V/V_{max} weight. We also built control samples from the galaxies not included in the pair selection criteria, as counterparts for both the LSBGs and HSBGs pairs; the control galaxies have the same absolute magnitude distribution as the those in pairs (see Figure 6).

Now that we ensure that the population of LSB and HSB pairs are comparable, we can search for trends between the star-forming parameters and the environment properties, such as the local density. The upper panels of Figures 7 and 8 show the distributions of the birthrate parameter b (Fig. 7) and the D_n4000 index (Fig. 8), for the sample of pairs and the control sample. Both distributions are defined above (respectively, below for Fig. 8) a threshold value from which we can naturally define those systems with a high star-forming activity (respectively, very recently formed stars for Fig. 8). In this case we choose pairs with $b > 1.8$ and $D_n4000 < 1.3$. These systems, clearly with star-forming processes and/or recently formed stars, are worth to be characterized in terms of the projected distance to the closest neighbor r_p, normalized by the Petrosian radius r_{90}. Results can be observed in lower panels of Figures 7 and 8, where we plot the average birthrate parameter b and the D_n4000 index as a function of the r_p/r_{90} ratio. The blue dot-dashed lines represent the corresponding fractions and averages for the control sample for both groups of galaxies. Note that in these two figures, both the fractions and averages are weighted by V/V_{max}. Figure 7 shows an increase in the stellar formation activity for HSBGs compared to the corresponding control sample. This is in agreement with previous works (O'Neil et al. 2007, and references therein). Regarding the LSBGs, both the control sample of LSBGs and the LSBGs with pairs, exhibit

a significant fraction of galaxies with star forming processes (around 30%). This increases even more for pairs with $r_p/r_{90} \leq 4$, where the fraction of star-forming galaxies doubles, to reach up to 60%, which represents a large value when compared to that for the control sample. Note that for the average birthrate parameter b, $< b >$, we observe an increment in the first bin of r_p/r_{90}, twice as large as the increment in the same bin observed for the LSBG pair sample. This behavior is mainly due to the fact that the b distribution for the HSB galaxies dominates for $b > 4$, which *is not* the case for the LSB galaxies (then the difference in the $< b >$ value for HSBGs and LSBGs).

On the other hand, the increase of the star formation signatures described above is consistent with the fraction of young stars from the D_n4000 index distribution (Figure 8). Both samples of galaxies (LSBGs and HSBGs), exhibit an increase in the fraction of galaxies having recent star formation episodes, when r_p/r_{90} decreases, in comparison with the corresponding control samples (the horizontal blue dot-dashed lines). The smaller average values of $<D_n4000>$ for LSBGs compared to HSBGs for $r_p/r_{90} > 10$, indicate that LSBGs in average have *younger* stellar populations than HSBGs at large separation scales. In fact, results show that in average, the fraction of young stars in LSBGs is roughly similar for all scales. Note that for both LSBGs and HSBGs the average value for D_n4000 is smaller than the corresponding value for the control sample.

4.3. The AGN and LSB connection

There are several reasons for devoting special attention to the fraction of LSBGs which host AGN activity. First, the evolution of an AGN can alter the evolution of the entire galaxy (Silverman et al. 2008, and references therein). Second, it has been claimed (Galaz et al. 2002) that the bulge size can be related to the metallicity, where smaller bulges are metal poor, favoring a secular evolution picture for the case of some barred spiral LSBGs and clearly appealing to the mass metallicity relationship in non-barred spirals (Lagos, Padilla & Cora 2009). Concerning the fraction of LSBGs hosting AGNs, Sprayberry et al. (1995b) found that *half* of his sample of 10 giant LSBGs exhibit AGNs. The same fraction was also found by Schombert (1998). These rather high fractions were challenged by Impey et al. (2001), who found that only 5% of their LSB sample, selected from the Automated Plate Measuring Machine Survey (Maddox et al. 1990, APM), hosted AGNs. Finally, Mei et al. (2009), using 194 LSBGs from the spectroscopic catalog of Impey et al. (1996), along with spectroscopic information from the SDSS DR 5, concluded that 10%-20% of the LSBGs host an AGN, to be compared to the 40%-50% of HSBGs presenting an AGN.

The luminosity of the bulge has also an important role in the fraction of spirals with an

AGN. Schombert (1998) using a sample of galaxies with high HI emission concluded that the occurrence of AGN was highest in systems with bulges, regardless of morphological type or mean surface brightness. However, the existence of a stellar population (and the associated gravitational gradient) appears to be a prerequisite for an active nuclear region. This evidence points to other results indicating that the bulge and disk evolution are decoupled and so whatever star formation processes produced the bulges did not affect the disks (Das et al. 2009).

Motivated by the above, we devote attention to the HSBGs and LSBGs hosting an AGN. The sample of galaxies hosting an AGN, for both samples containing LSBGs and HSBGs, was obtained using the Kauffmann et al. (2003) catalog, using the well-known BPT diagnosis diagram (Baldwin, Phillips & Terlevich 1981) from the intensity of the [OIII]λ5007, Hβ, [NII]λ6583 and Hα lines. Following the BPT diagram, AGNs are defined as galaxies having

$$\log([OIII]/H\beta) \geq 0.61/(\log([NII]/H\alpha) - 0.05) + 1.3. \quad (4)$$

Using the above selection criterion, 495 out of 9,421 LSBGs present an AGN. On the other hand, 5,677 HSBGs out of a total of 30,000 also exhibit an AGN. In rough numbers then, 19% of the HSBGs present an AGN, compared to the 5% of the LSBGs having an AGN. Figure 9 shows the fraction of HSBGs and LSBGs in our sample presenting AGNs, as a function of the redshift, the absolute magnitude in the r-band, the log of the stellar mass, and the Petrosian radius r_{90} in kpc. Both in the HSB and LSB galaxies, we observe that the redshift distributions *and* the absolute magnitude distributions for both LSBGs and HSBGs are similar. This is expected since both AGNs and LSBGs are detected in the brightest portion of absolute magnitude range. A similar distribution is also observed in the stellar mass distribution for both the LSBGs and HSBGs having AGNs (left bottom panel). Where things are clearly different is in the size distribution of HSBGs and LSBGs having an AGN (right bottom panel). Although both distributions are similar in shape, LSBGs hosting an AGN are larger, in average, than the HSB counterparts. Also, when comparing r_{90} between Figure 9 and Figure 2 (or Figure 3), it is worth noting that both LSBGs and HSBGs hosting an AGN are *smaller* in average than the counterparts lacking an AGN. We suggest that the presence of an AGN could be responsible for this difference observed statistically.

In Figure 10 we compare the color properties of LSBGs and HSBGs with and without AGN, via the $U - B$ vs. $B - V$ color-color diagram (LSBGs in the left panel, and HSBGs in the right panel). Black points represent the galaxies without AGN and the green points represent galaxies hosting an AGN. For both HSBGs and LSBGs, galaxies having an AGN are in average redder than their counterparts lacking an AGN. The average values for LSBGs

having an AGN is $U - B = 0.23 \pm 0.01$ and $B - V = 0.85 \pm 0.01$. This locates the LSBGs-AGN galaxies in the space covered mainly by the red population of LSBGs (delimited by the red line), a region first noted by O'Neil et al. (1997), and reinforced by Galaz et al. (2002) who show, using near-IR photometry, that a large fraction of LSBGs with high gas fractions host old and red stellar populations.

The fraction of LSBGs and HSBGs with AGN, as a function of the absolute magnitude and the log of the stellar mass, is shown in Figure 11. In agreement with the previous authors already cited, the fraction of LSBGs hosting an AGN is always lower than the corresponding fraction of HSBGs also hosting an AGN, regardless of the absolute magnitude and the stellar mass. It is not surprising that both parameters evolve in the same way (larger fraction of AGNs for brighter objects and larger masses), since both quantities are related via the mass-luminosity relation. As this Figure shows, the AGN fraction is a steep function of the brightness (and the mass) of the galaxy, as observed by many authors (Hopkins et al. 2007, and references therein). As it has been claimed, this is just another realization that the mass of the black hole (and then the power of the AGN), is related to the mass of the galaxy itself (Marconi & Hunt 2003, and references therein). For the lowest covered masses ($\sim 10^{9.8}$ $M_{\odot}$), the fraction of LSBGs hosting an AGN is $\sim 5\%$, roughly the same fraction observed for the HSBGs. However, for the larger masses covered by this statistics, the fraction of LSBGs hosting an AGN reaches $\sim 30\%$, which is 10% *lower* than the corresponding fraction of HSBGs hosting an AGN. These fractions are quite similar when using the absolute magnitude. Why, regardless the stellar mass of a galaxy, the fraction of LSBGs hosting an AGN is lower than the fraction of HSBGs having AGNs? This may be related to the star formation properties of LSBGs in different environments described in §4.2, a subject we discuss in §5.

Regarding the bulge luminosity and the fraction of galaxies with AGN, we obtain similar results for the two galaxy populations (HSBGs and LSBGs). Figure 12 shows the fraction of LSBGs and HSBGs with AGN as a function of the parameter used to define the luminosity contribution of the bulge (i.e. the fracDev parameter), represented by a de Vaucouleurs luminosity profile. Both distributions are normalized by the total number of galaxies of the same population found in each bin of fracDev. The black and red lines show the trend for the HSBGs and the LSBGs, respectively. It is apparent that both fractions increase (with almost the same slope) as the bulge dominates the galaxy luminosity, a result in agreement with other works discussed here (Schombert 1998, and references therein). We see also that the HSBG population has a larger fraction of AGN compared to LSBG counterparts, in agreement with the fact that the HSBGs host a larger fraction of AGN than the LSBG counterparts (19% for the HSBGs and 5% for the LSBGs). In order to check the morphology of the galaxies with AGN, we examined by eye the HSBGs and LSBGs hosting an AGN. Both populations show exclusively spiral galaxies with a visible bulge, the LSBGs-AGN exhibiting

bluer colors than the HSBG-AGN population and less prominent bulges (see Figure 13). However, the LSBG-AGN population has a larger fraction of small bulges. These galaxies have spectra with less prominent AGN signatures compared to those with more luminous bulges. All this evidence is in agreement with the trend observed in other AGNs, where there is a close relationship between the bulge luminosity and the power of the AGN, represented by the emission line diagnosis.

5. Discussion

As argued in the introduction, there is still a debate about the evolution of LSBGs when located in dense environments. Are LSBGs destroyed in dense environments, or they just change their condition of LSBGs, turning into HSBGs? Given that these galaxies dominate the volume density of galaxies (Dalcanton et al. 1997), then having clues to solve this issue is of fundamental importance. There are basically two different scenarios describing the evolution of an LSBG in dense environments, especially when an LSBG is subject to the direct influence of another galaxy. The first scenario establish that LSBG disks are unstable under perturbations (given their low density), making LSBGs very sensitive to the local density and hence making them to populate only low density environments. A second scenario, also supported by models (Mihos et al. 1997, hereafter MMB model) and observations (Pickering et al. 1997; Das, Boone & Viallefond 2010), yields *stable disks against interactions*, for sufficiently *low* stellar mass densities (Σ_s) and assuming large amounts of dark matter, as it is the case for LSBGs. In this picture, below a mass density threshold, perturbations generated by the interactions would be unable to be amplified, preventing the galaxy from being destroyed and/or producing significant star formation episodes. The net result is a much more stable galaxy against close interactions. Such a stability would be represented, for example, by the lack of bars and the absence of flow of material which can form stars or even feed a central massive black hole (activating an AGN). Therefore, the deficit of LSBGs hosting AGNs, compared to those found in HSBGs, could fit at least with the picture the MMB model presents.

This last picture also fits well, but with a subtlety, with the values of the stellar formation indexes $< b >$ and $<\mathrm{D}_n4000>$ as a function of the interacting distance r_p/r_{90}, as found for both LSBGs and HSBGs (Figures 7 and 8). When comparing the fraction of LSBGs and HSBGs with the *highest* values of b ($b > 1.8$), we realize that these fractions are the same at all scales, for the whole range of r_p/r_{90}; i.e., there is no distinction in the star forming properties between LSBGs and HSBGs, where the latter are actively forming stars. However, when looking at the complete range of b, we discover that at smaller scales (i.e. close interactions,

$r_p/r_{90} < 5$), the fraction of HSBGs having stellar formation episodes *double* that of LSBGs. These results could match the two scenarios described above. In one case, the lack of LSBGs with high values of b (significant stellar formation episodes) points to the possibility that such galaxies could no longer be LSBGs, having evolved to a higher surface brightness regime. On the other hand, following the MMB model, the difference in the interaction signature could be explained by the disk stability, preventing LSBGs from changing their star formation rate, as it is observed in HSBGs.

Thus, our results support the picture where LSBGs are more isolated than HSBGs at large scales, a result in agreement with those by Rosenbaum et al. (2009). However, more than the local density value, are the interactions with close neighbors which actually make LSBGs evolve. Interestingly, when this occurs, LSBGs seem to be more stable than HSBGs, preventing LSBGs to change significantly their stellar formation signatures as usually expected with respect to HSBGs with close companions. This last behavior, together with the lower fraction of LSBGs with AGNs compared to the fraction of HSBGs also hosting AGNs (for the full mass range), could be explained by the difficulty shown by interacting LSBGs to form bars, lacking the natural bridge which transports material to the center of the galaxy, preventing the central black hole from being fueled, and then remaining the galaxy as a non-AGN.

6. Conclusions

Our conclusions can be summarized as follows.

- For a sample of 9,421 LSB galaxies selected from the SDSS DR 4 (1.66% of a total of 567,486 galaxies), in the redshift range $0.01 < z < 0.10$, the cumulative distributions of the distance to the nearest and the fifth closest neighbors, indicate that LSBGs are more isolated than high surface brightness galaxies (HSBGs). Also, LSBGs specially avoid high density environments, i.e. are almost completely *unpopular*, following the Bothun et al. (1993) terminology. When describing the degree of isolation in terms of the surface density of galaxies, our results yield a deficit of neighbors for LSBGs at small scales (<1 Mpc). For larger scales ($\geq$ 2.5 Mpc), we obtain consistent fractions of LSBGs and HSBGs. This is in fairly good agreement with results by Rosenbaum et al. (2009). However, we do not detect a higher degree of isolation of LSBGs in the scale range 2-5 Mpc as these authors do. This difference can be explained by the different galaxy selection criteria, as most of our galaxies are spirals, losing some spirals with extremely bright bulges *and* faint disks, as well as faint irregulars ($M_r > -16.0$ mag), and Rosenbaum's low redshift ones are mostly dwarfs.

- The fraction of LSBGs with high stellar formation signatures and/or a high population of recently formed stars, increases when galaxies are close to a neighbor ($r_p/r_{90} \leq 4$), and is clearly larger when compared to a sample of isolated LSBGs. This behavior is similar in HSBGs also suffering interactions. However, when comparing the average value of the stellar formation signature (e.g. the birthrate parameter b), interacting HSBGs form *twice* the stars as the interacting LSBGs. This last difference could be explained by models of Mihos et al. (1997, MMP models), which show the difficulty of low density stellar disks (i.e. low surface brightness disks) surrounded by significant dark matter haloes, to amplify and propagate perturbations due to close companions.

- The fraction of LSBGs hosting an AGN is lower than the fraction of HSBGs with AGNs. 5% of the LSBGs host an AGN, compared to the 19% of the HSB systems. These two fractions are in agreement to those found by Impey et al. (2001). This is systematic for the whole range of masses covered in this work (i.e. for the whole range of absolute magnitudes of the volume-limited sample, $-22.0 < M_r < -19.8$). This could be explained by the difficulty of LSBGs to react under close companions (MMP models), which would produce a deficit of bars and other structures in LSBGs capable to transport material to activate the massive central black hole, which when active, would generate an AGN. Another interesting result is obtained when the frequency of an AGN is compared between the LSBG and HSBG populations, in terms of the bulge optical luminosity. We obtain that for both the HSBG and the LSBG populations, the fraction of AGNs increases with the bulge luminosity with almost the same slope, in agreement with other authors.

As a general conclusion, this study suggests that, rather than being a condition for their formation, isolation of LSBGs is more connected to their survival and evolution.

This research is supported by FONDECYT grant 1085267, by FONDAP Center for Astrophysics 15010003, and BASAL CATA. GG thanks the Department of Astronomy, University of Washington, Seattle, and the Department of Astronomy of the University of Maryland, at College Park, for their welcome during the writing of this paper. In particular, GG acknowledges Julianne Dalcanton for the fruitful discussions on the subject covered by this work. The authors are grateful to the anonymous referee who helped to improve the form and content of this paper.

Funding for the SDSS and SDSS-II has been provided by the Alfred P. Sloan Foundation, the Participating Institutions, the National Science Foundation, the U.S. Department of Energy, the National Aeronautics and Space Administration, the Japanese Monbukagakusho, the Max Planck Society, and the Higher Education Funding Council for England. The

SDSS Web Site is http://www.sdss.org/. The SDSS is managed by the Astrophysical Research Consortium for the Participating Institutions. The Participating Institutions are the American Museum of Natural History, Astrophysical Institute Potsdam, University of Basel, University of Cambridge, Case Western Reserve University, University of Chicago, Drexel University, Fermilab, the Institute for Advanced Study, the Japan Participation Group, Johns Hopkins University, the Joint Institute for Nuclear Astrophysics, the Kavli Institute for Particle Astrophysics and Cosmology, the Korean Scientist Group, the Chinese Academy of Sciences (LAMOST), Los Alamos National Laboratory, the Max-Planck-Institute for Astronomy (MPIA), the Max-Planck-Institute for Astrophysics (MPA), New Mexico State University, Ohio State University, University of Pittsburgh, University of Portsmouth, Princeton University, the United States Naval Observatory, and the University of Washington.

REFERENCES

Abazajian K. et al. 2004, AJ, 128, 502

Alonso M.S., Lambas D. G., Tissera P.B., Coldwell G., 2006, MNRAS, 367, 1029

Baldwin, J. A., Phillips, M. M. Terlevich, R., 1981, PASP, 93, 5

Brinchmann J. et al. 2004, MNRAS, 351, 1151

Balogh M. et al, 2004, MNRAS, 348, 1355

Bothun, G., Schombert, J., Impey, C., Sprayberry, D., McGaugh, S. 1993, AJ, 106, 530

Bothun, G. D., Impey, C. D., Malin, D. F., Mould, J. R. 1987, AJ, 94, 23

Dalcanton, J., Spergel, D., Gunn, J., Schmidt, M., Schneider, D. 1997, AJ, 114, 635

Das, M., Boone, F., & Viallefond, F. 2010, A&A, accepted, arXiv:1006.1973

Das, M., Reynolds, C., Vogel, S., McGaugh, S., Kantharia, N. 2009, ApJ, 693, 1300

de Blok, W. 2005, ApJ, 634, 227

de Blok, W. J. G. & McGaugh, S. S. 1996, ApJ, 469, L89

Freeman K. C. 1970, ApJ, 160, 811

Galaz, G., Cortes, P., Bronfman, L., & Rubio, M. 2008, ApJ, 677, L13

Galaz, G., Dalcanton, J., Villalobos, A., Infante, L., & Treister, E. 2002, AJ, 124, 1360

Hopkins P.F., Hernquist L., Cox T.J., Robertson B. & Krause E. 2007, ApJ, 669, 67

Impey, C. D., Burkholder, V., Sprayberry, D. 2001, AJ, 122, 2341

Impey, C. D., Sprayberry, D., Irwin, M. J., Bothun, G. D. 1996, ApJS, 105, 209

Kauffmann G. et al. 2003, MNRAS, 346, 1055

Lagos, C., Padilla, N., & Cora, S. 2009, MNRAS, 97, L31

Lambas D. G., Tissera P.B., Alonso M.S., Coldwell G. 2003, MNRAS, 346, 1189

de Lapparent, V., Arnouts, S., Galaz, G., Bardelli, S. 2004, A&A, 422, 841

Maddox, S. J., Efstathiou, G., Sutherland, W. J.;,Loveday, J. 1990, MNRAS, 243, 692

Marconi, A., & Hunt, L. 2003, ApJ, 589, L21

Matthews, L. D., & Gao, Y. 2001, ApJ, 549, L191

Mayer, L., & Wadsley, J. 2004, MNRAS, 347, 277

Mihos, J.C., McGaugh, S. S., de Blok, W. J. G. 1997, ApJ 477, L79

Mei, L., Yuan, W., Dong, X., 2009, Research in Astronomy and Astrophysics, 9, 269

Nikolic B., Cullen H., Alexander P. 2004, MNRAS, 355, 874

O'Neil, K., Oey, S., Bothun, G. 2007, AJ, 134, 547

O'Neil, K., Hofner, P., & Schinnerer, E. 2000 ApJ 545 L99

O'Neil, K. Bothun, G., Schombert, J., Cornell, Mark E., Impey, C. 1997, AJ, 114, 2448

Padilla, N., Lambas, D.G., & González, R., 2010, MNRAS, in press

Pickering, T., Impey, C., van Gorkom, J., & Bothun, G. 1997, AJ, 114, 1858

Rosenbaum, S., Krusch, E., Bomans, D, & Dettmar, R. 2009, A&A, 504, 807

Rosenbaum, S. D., Bomans, D. J., 2004, A&A, 422, L5

Schmidt, M. 1968, ApJ, 151, 393

Schombert, J. 1998, AJ, 116, 1650

Smith J. A. et al. 2002, AJ, 123, 2121

Silverman, Mainieri, V., Lehmer, B. et al. 2008, ApJ, 675, 1025

Sprayberry, D., Bernstein, G., Impey, C., & Bothun, G. 1995a, ApJ, 438, 72

Sprayberry, D., Impey, C. D., Bothun, G. D., Irwin, M. J. 1995b, AJ, 109, 558

Strauss M. et al. 2002, AJ, 124, 1810

van den Hoek, L., de Blok, W., van der Hulst, J., de Jong, T. 2000, A&A, 357, 397

Swaters, R., Sanders, R., & McGaugh, S. 2010, 718, 380

Zackrisson, E., Bergvall, N., & Ostlin, G. 2005, 435, 29

Zhong G.H. et al. 2008, MNRAS, 391, 986

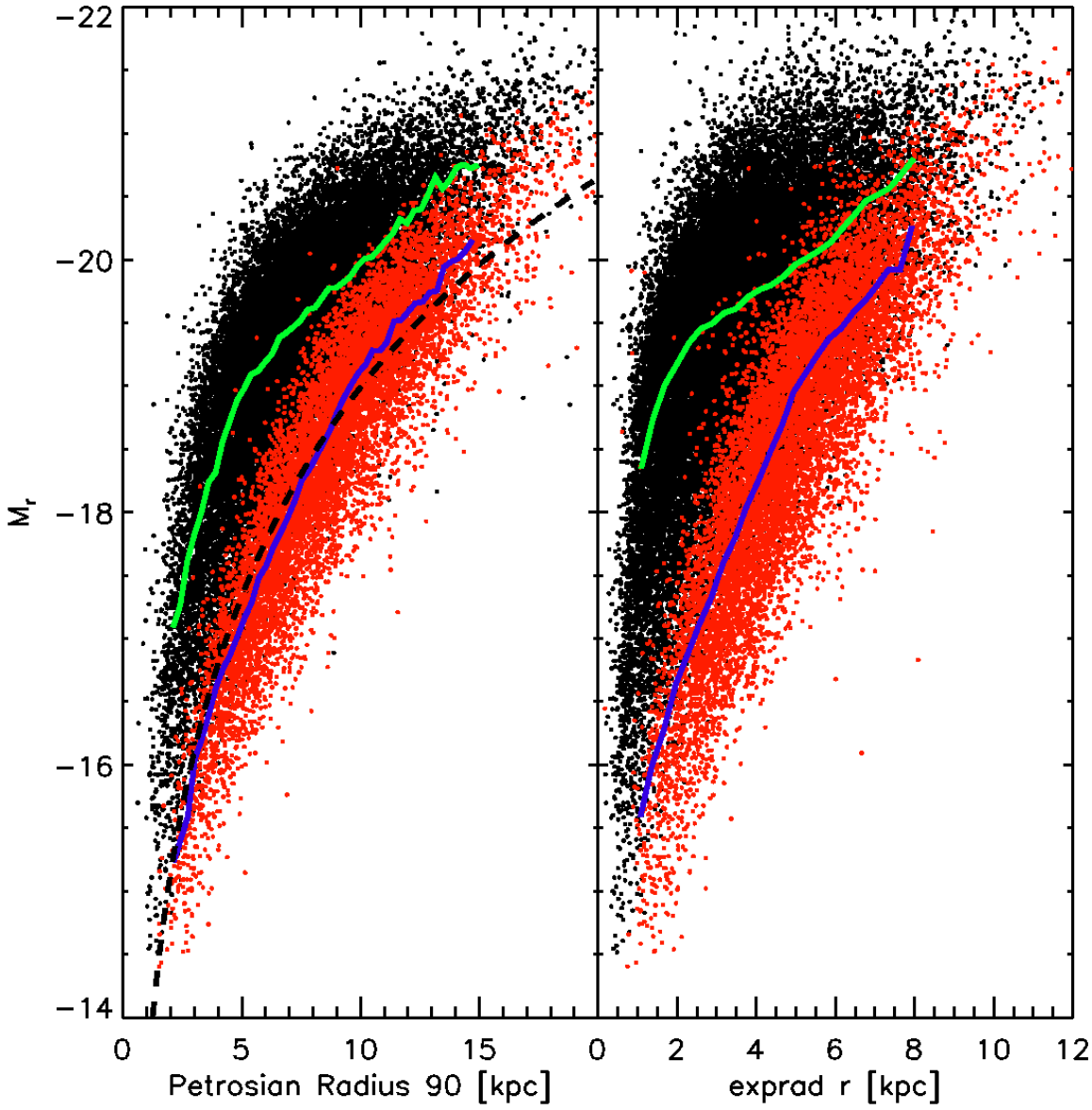

Fig. 1.— In black HSBGs and in red LSBGs. Left panel: Absolute magnitude in the r band vs. the Petrosian radius including 90% of the light. Right panel: the same absolute magnitude but as a function of the exponential scale length measured in kpc. Black dashed line indicates the region where 90% of the galaxies are LSBGs; Green and blue lines correspond to the median for HSBGs and LSBGs, respectively.

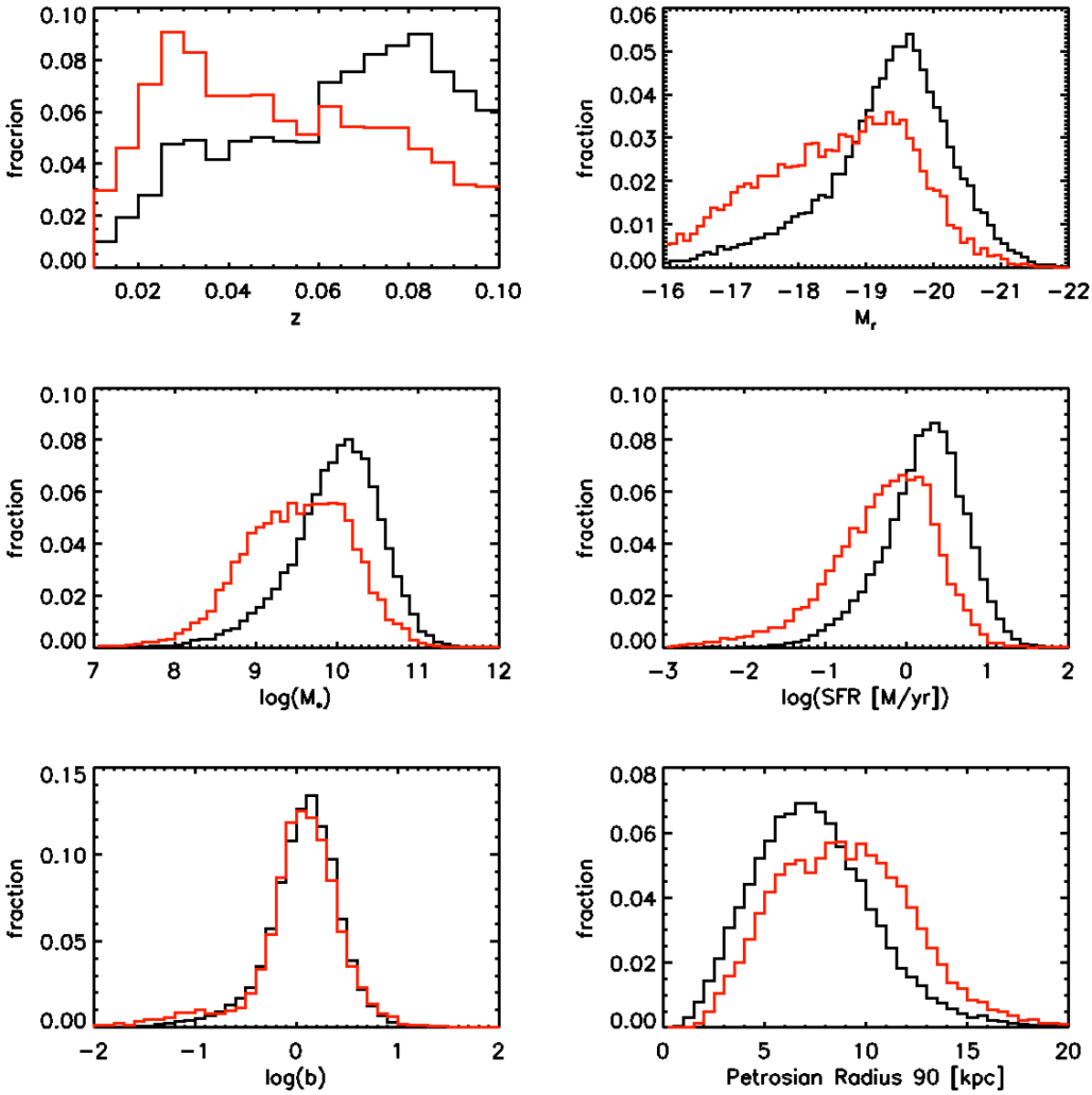

Fig. 2.— V/V_{max} weighted distributions of galaxy properties for our sample of LSBGs (red) and HSBGs (black). From up to bottom, from left to right: the redshift (z) distribution, the absolute magnitude in the r band, the log of the stellar mass (M_*), the log of the star formation rate, in solar masses per year ($M_\odot$/year), the log of the birthrate parameter b, and the Petrosian radius with 90% of the galaxy light (r_{90}). The observed distributions have been corrected from volume incompleteness by the factor V/V_{max}. See text for details.

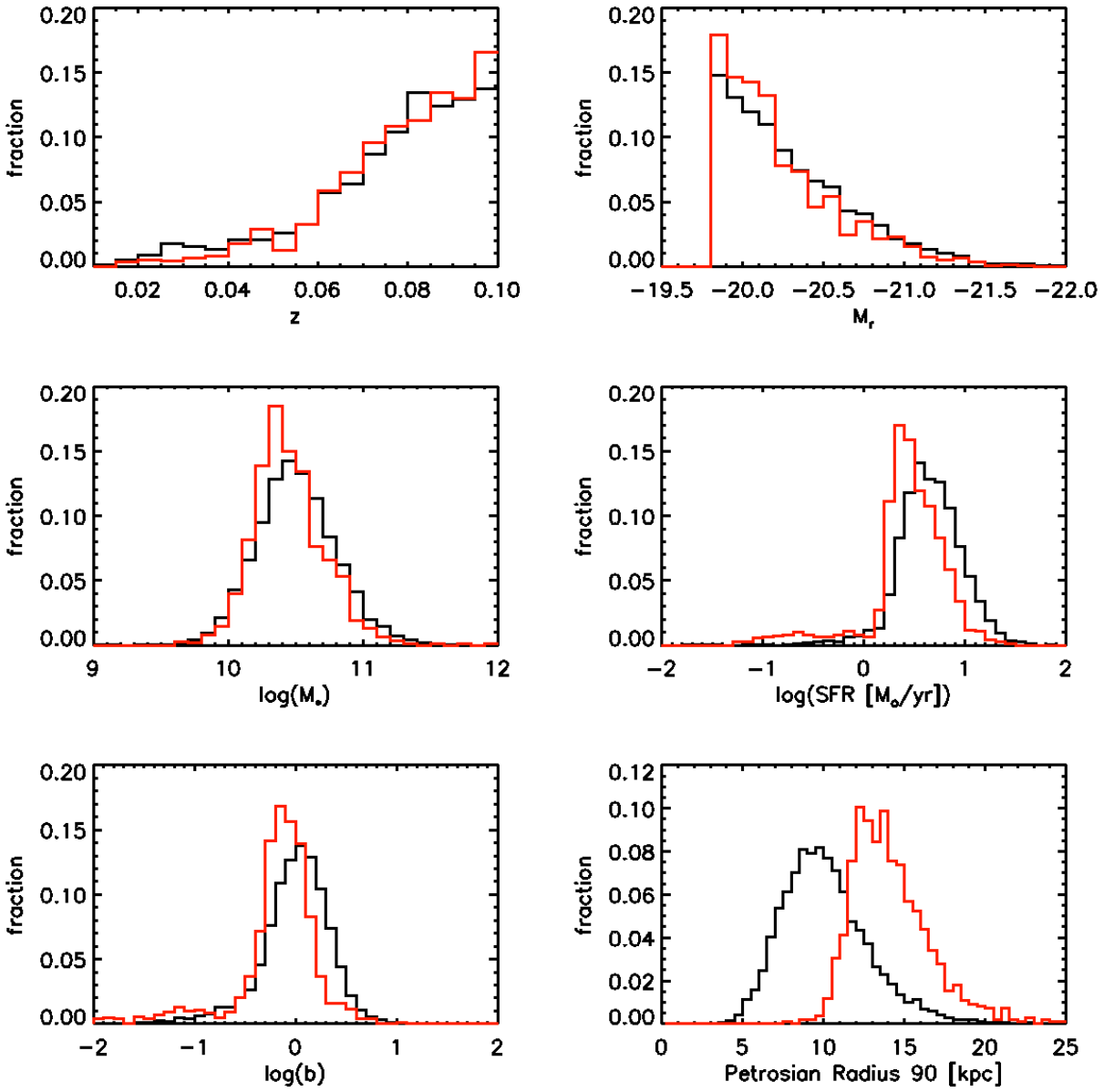

Fig. 3.— In red, LSBGs; in black, HSBGs. Same as Figure 2 but now considering only the volume-limited catalog. We see that the redshift and absolute magnitude distributions are heavily modified. See text for details.

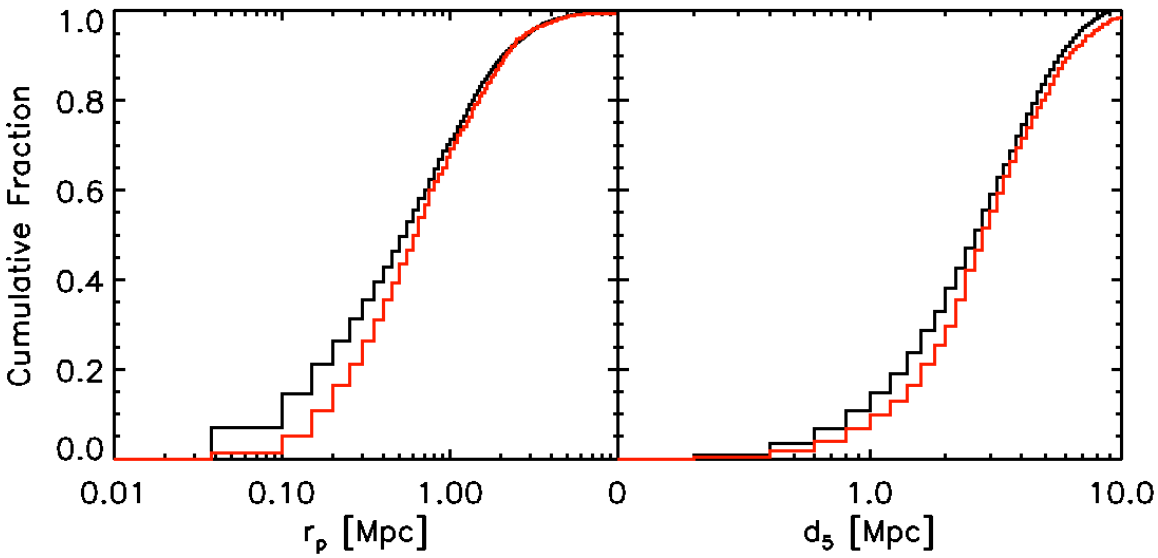

Fig. 4.— Cumulative distribution of the first (left panel) and fifth (right panel) nearest neighbor, for LSBGs (red) and HSBGs (black). Note that LSBGs always have a smaller number of neighbors than HSBGs, at all scales, but more significantly for scales smaller than ~ 4 Mpc for d_5. See text for a detailed discussion.

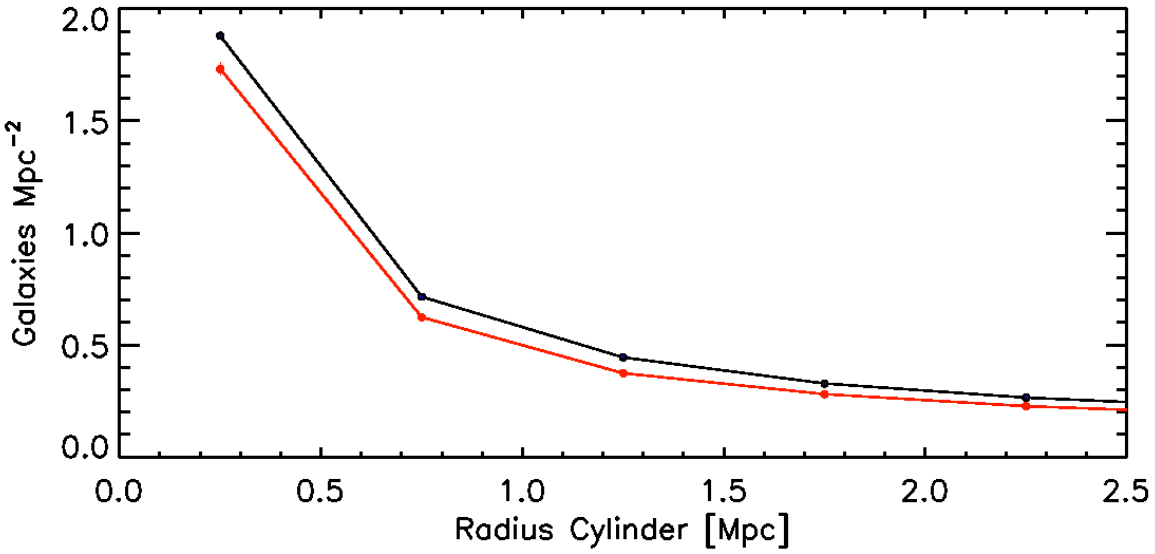

Fig. 5.— Surface density of neighbors around LSBGs (red) and HSBGs (black) as a function of the radius of the cylinder. Note that error bars are of similar size as the symbol size. This estimator also indicate that LSBGs are more isolated than HSBGs.

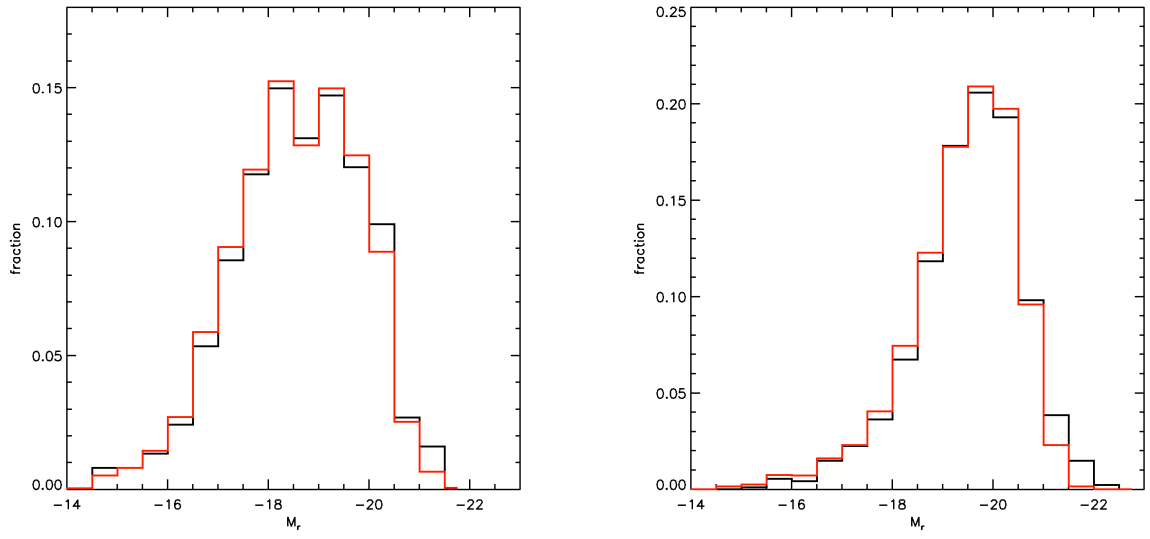

Fig. 6.— Absolute magnitude distributions for interacting LSBGs (left panel, black line) and interacting HSBGs (right panel, black line). The red lines correspond to the absolute magnitude distributions for the control non-interacting galaxies. See text for details about how these samples are built.

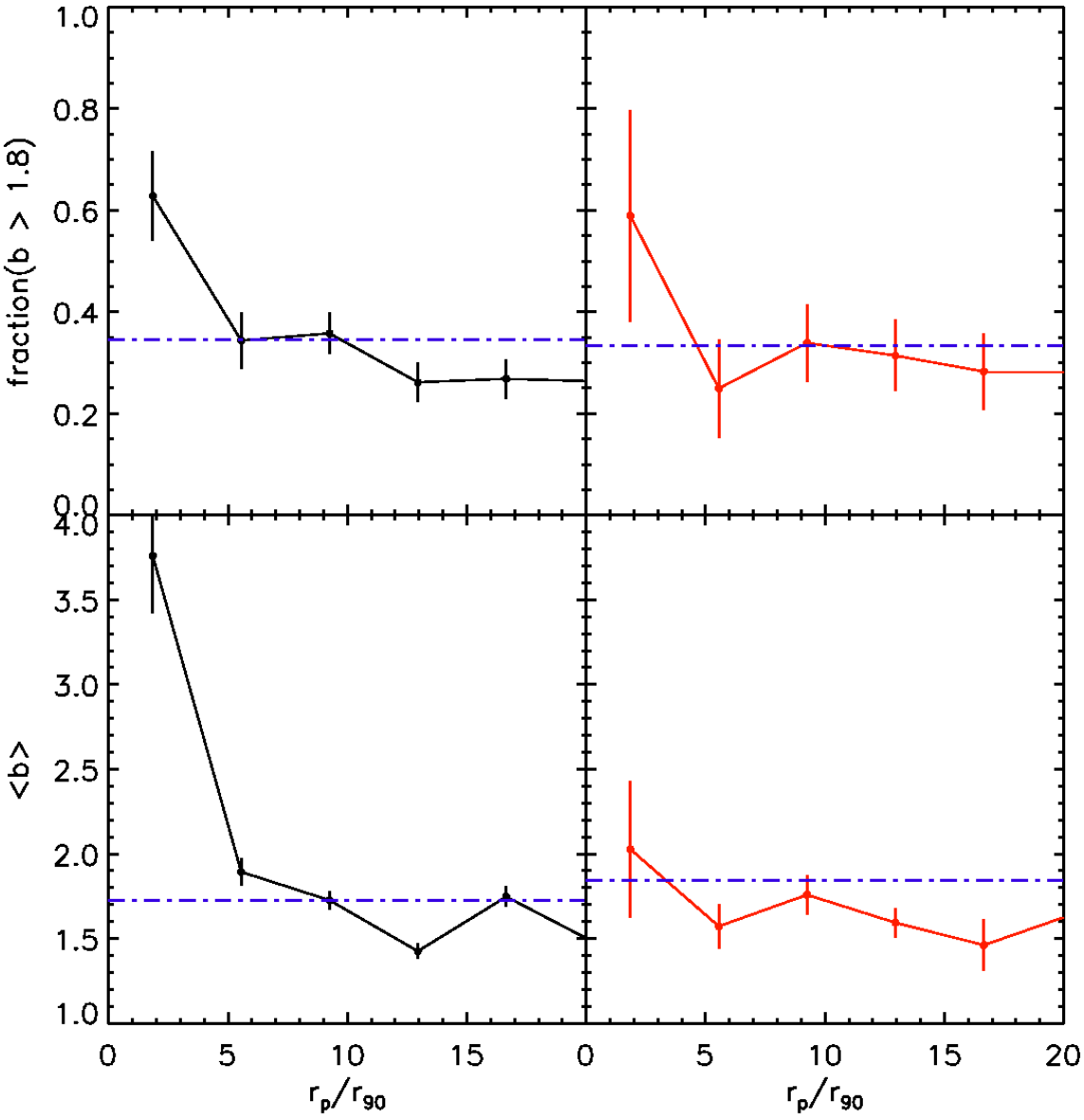

Fig. 7.— Upper panel: V/V_{max} weighted fraction of galaxies with significant stellar formation activity (birthrate parameter $b \geq 1.8$), as a function of the distance parameter to the nearest neighbor r_p/r_{90}. Lower panels: the V/V_{max} weighted value of $< b >$ for galaxies, as a function of r_p/r_{90}. Left panels are for the HSB case and right panels for the LSB case. See text for details and conclusions from this Figure.

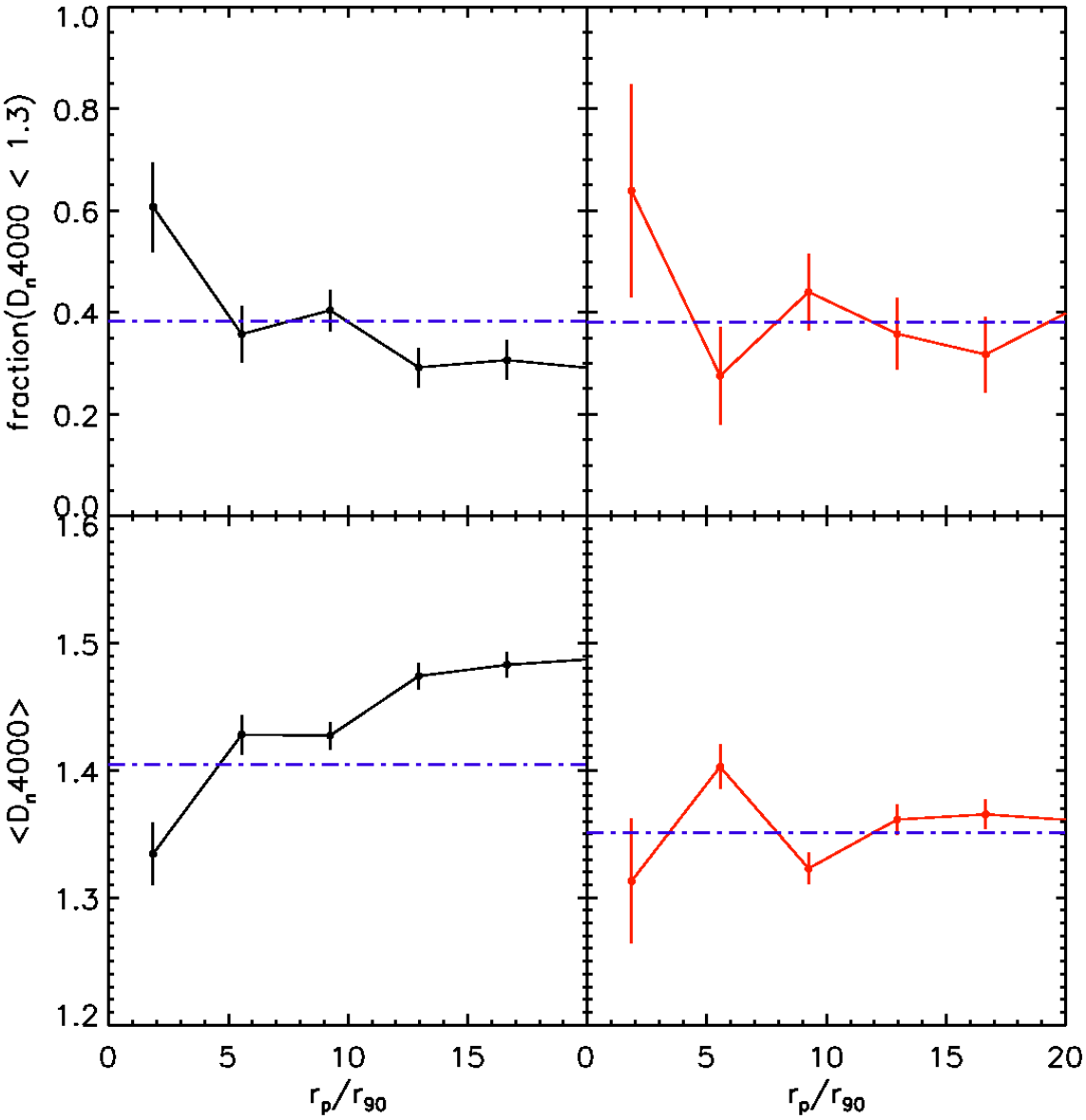

Fig. 8.— Upper panel: V/V_{max} weighted fraction of galaxies with very recently formed stars (D_n4000 index smaller than 1.3), as a function of the distance parameter to the nearest neighbor r_p/r_{90}. Lower panels: the V/V_{max} weighted value of $<D_n4000>$ for galaxies, as a function of r_p/r_{90}. The black lines denote the HSB case and the red lines the LSB case. See text for details and conclusions from this Figure.

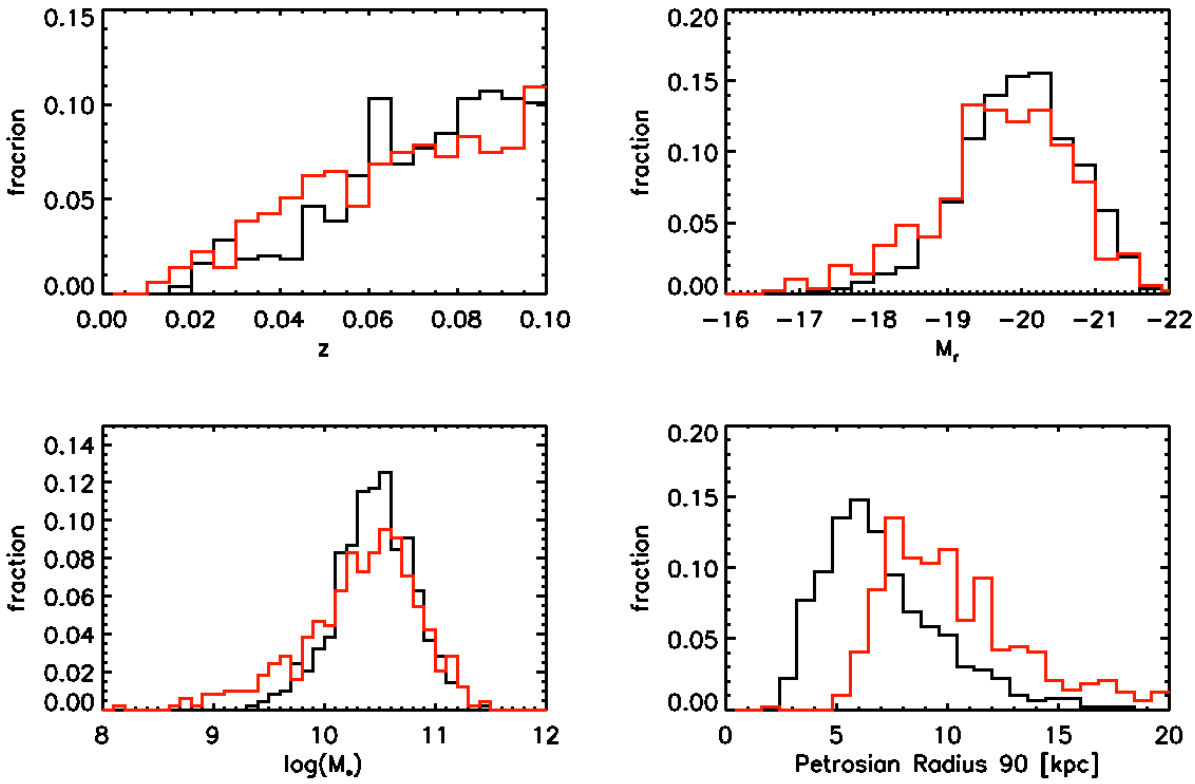

Fig. 9.— Histograms for the LSBGs (red) and HSBGs (black) hosting an AGN. From the upper panel to the right to the bottom: redshift z, absolute magnitude in the r band, log of the stellar mass, and the Petrosian radius r_{90}. Most of the distributions for LSBGs and HSBGs with AGN are similar, except the distribution for the sizes given by the Petrosian radius. See text for details.

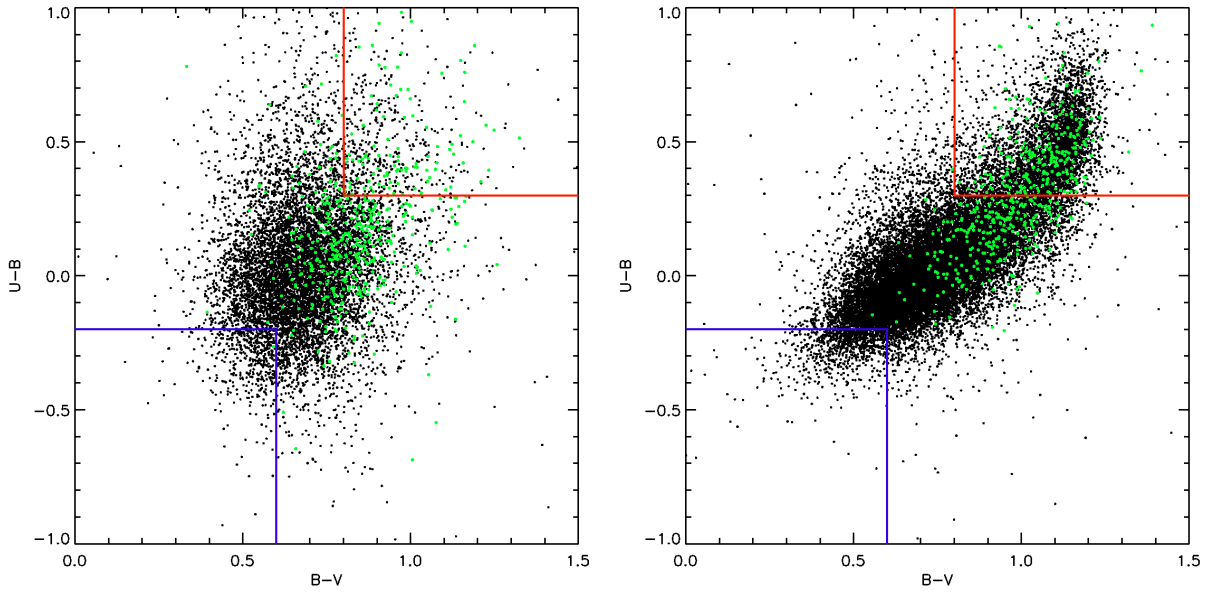

Fig. 10.— $B-V$ vs. $U-B$ color-color diagram of galaxies classified as LSBGs (left) and as HSBGs (right) from the SDSS data. The red and blue lines indicate what we define as "red" and "blue" galaxies, respectively. Green points are AGN-LSBGs. See text for details.

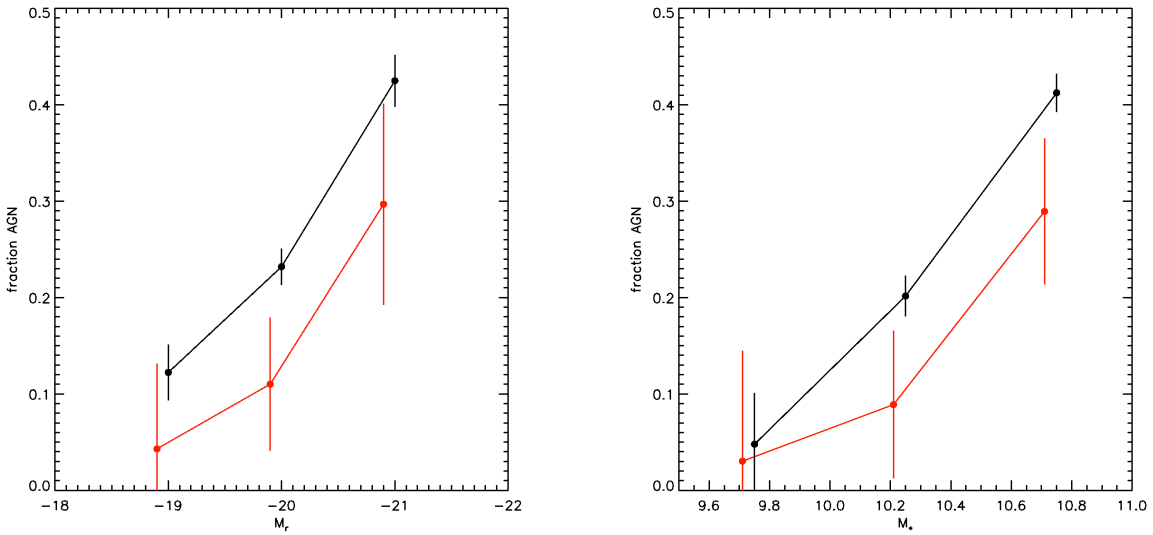

Fig. 11.— Fraction of HSBGs (black) and LSBGs (red) hosting an AGN, as a function of the absolute magnitude in the r band (left) and the stellar mass (right). For clarity, the x-axis of the LSBG sample has been slightly shifted to the left.

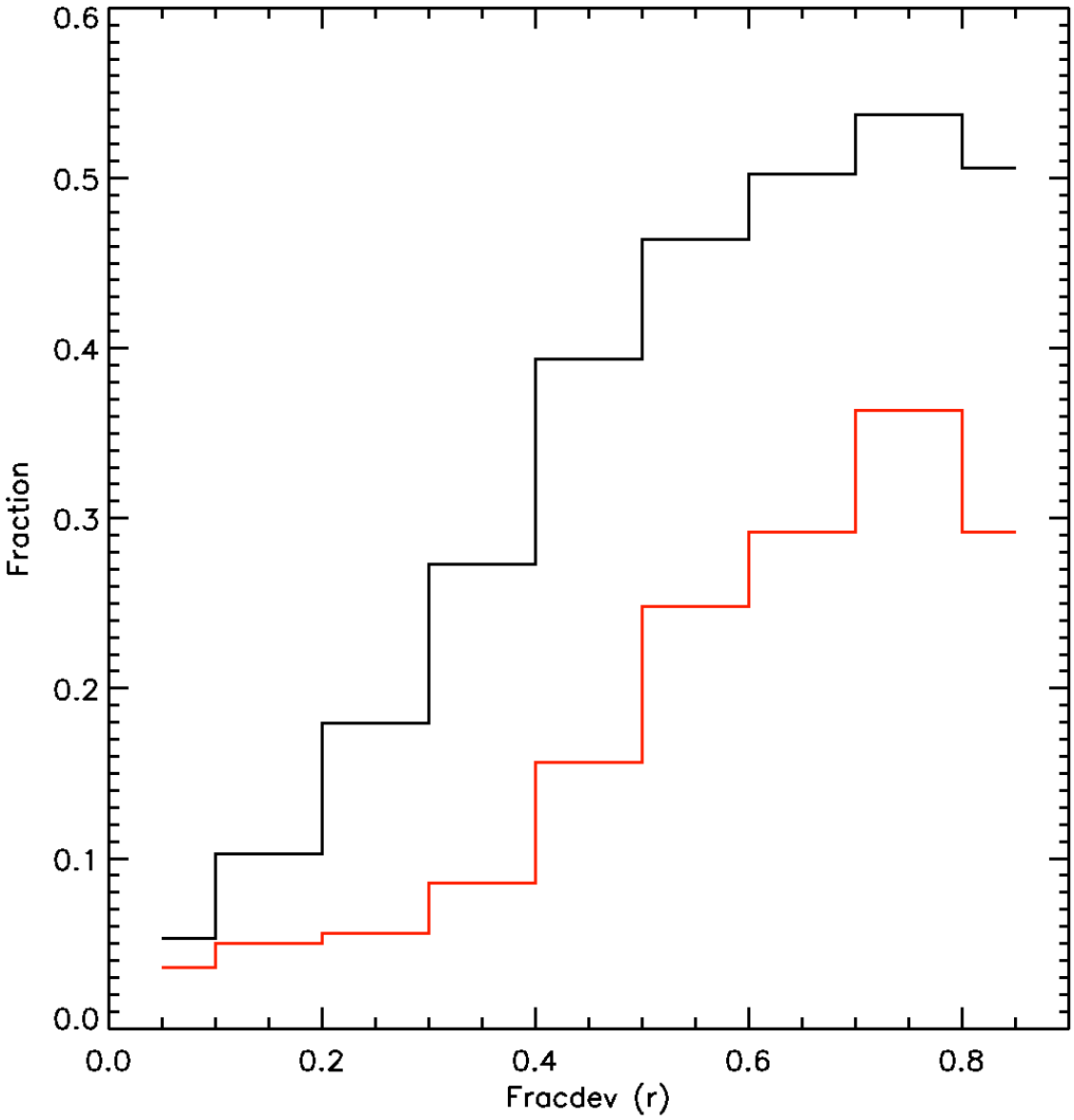

Fig. 12.— The fraction of HSBGs (solid line) and LSBGs (dashed line) having AGN as a function of the FRACDEV parameter, which represents the luminosity contribution of the de Vaucouleurs profile (or bulge profile). For both the HSBGs and the LSBGs populations, the fraction of galaxies hosting an AGN increases when the luminosity of the bulge increases. The fraction for each bin of fracDev is obtained by dividing the number of galaxies with an AGN in the given population in that bin, by the total number of galaxies of the same population in the same fracDev bin.

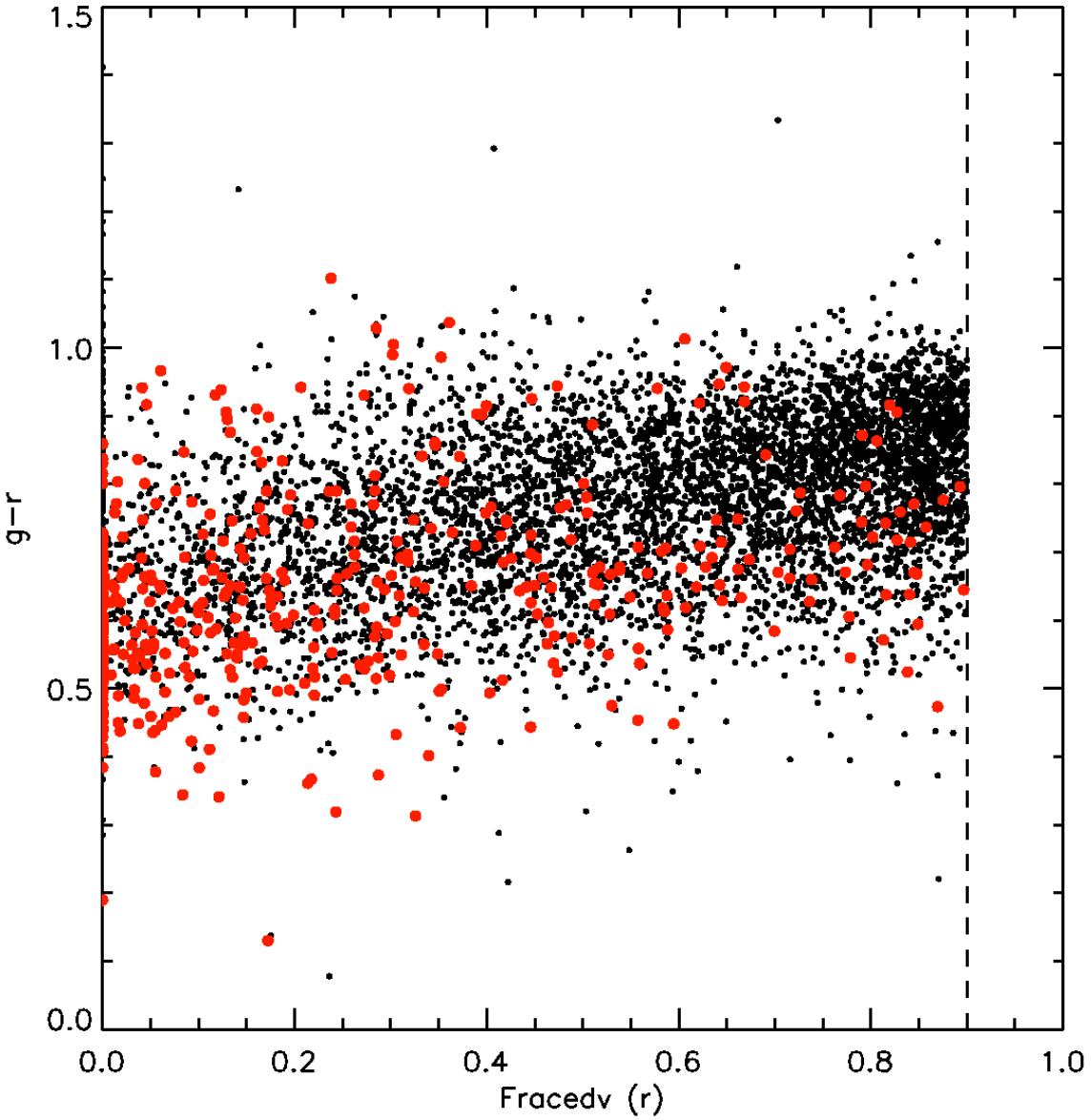

Fig. 13.— The color $g - r$ of the HSBGs (black) and LSBGs (red) hosting an AGN, as a function of the fracDev parameter representing the fraction of the total light given by the bulge. LSBGs tend to have smaller and less luminous bulges than HSBs. The vertical dashed line represents the limit in fracDev where the contamination by ellipticals begins to be significant.

Table 1. Averaged quantities for the V/V_{max} and volume-limited samples of LSBGs and HSBGs.

	V/V_{max} catalog		Volume-limited sample	
	HSB	LSB	HSB	LSB
z[1]	0.063 ± 0.001	0.051 ± 0.002	0.077 ± 0.001	0.079 ± 0.001
M_r[2]	-19.29 ± 0.01	-18.48 ± 0.01	-20.29 ± 0.01	-20.22 ± 0.01
M_*[3,4]	9.96 ± 0.08	9.46 ± 0.01	10.44 ± 0.01	10.43 ± 0.03
SFR[5,4]	0.15 ± 0.01	-0.46 ± 0.02	0.52 ± 0.02	-0.39 ± 0.03
b[6,4]	0.034 ± 0.01	-0.08 ± 0.02	-0.08 ± 0.01	-0.19 ± 0.02
r_{90}[7]	7.48 ± 0.02	8.99 ± 0.03	10.19 ± 0.03	14.24 ± 0.09
Numb. Galaxies[8]	30,000	9,421	7,526	1,110
Numb. AGN[9]	5,677	495	...	...

[1]Redshift.

[2]Absolute magnitude in the r band.

[3]Stellar mass, in solar masses ($M_\odot$).

[4]ogarithmic value (base 10).

[5]Star formation rate ($M_\odot$/yr).

[6]Birthrate parameter, expressed in star formation rate per unit of solar mass.

[7]Petrosian radius in kpc in the r-band, which encompasses 90% of the galaxy light.

[8]Number of galaxies in each sample.

[9]Number of galaxies of the corresponding sample, presenting an AGN. See text for details.

Table 2. Some averaged values for *isolated* and *popular* LSBGs and HSBGs in the sample.

	Isolated		Popular	
	HSBGs	LSBGs	HSBGs	LSBGs
M_r[1]	-20.35 ± 0.01	-20.32 ± 0.07	-20.34 ± 0.01	-20.21 ± 0.06
$g-r$[2]	0.68 ± 0.02	0.63 ± 0.02	0.52 ± 0.05	0.59 ± 0.01
b[3,4]	1.18 ± 0.04	1.1 ± 0.1	1.29 ± 0.04	0.9 ± 0.1
D_n4000[5]	1.55 ± 0.01	1.57 ± 0.03	1.53 ± 0.01	1.54 ± 0.03

[1]Absolute magnitude in the r-band.

[2]$g-r$ rest-frame color, from the SDSS DR 4.

[3]Birthrate parameter, expressed in star formation rate per unit of solar mass.

[4]ogarithmic value (base 10).

[5]D_n4000 index.